JOURNAL OF THE KOREAN ASTRONOMICAL SOCIETY
37: 593 ~ 596, 2004

FINDING COSMIC SHOCKS: SYNTHETIC X-RAY ANALYSIS OF A COSMOLOGICAL SIMULATION

ERIC J. HALLMAN[1,2], DONGSU RYU[3], HYESUNG KANG[4], AND T. W. JONES[1]
[1]Department of Astronomy, University of Minnesota, 116 Church Street SE, Minneapolis, MN 55455, USA
[2]Center for Astrophysics and Space Astronomy, University of Colorado at Boulder, 389 UCB, Boulder, CO 80309, USA
[3]Department of Astronomy & Space Science, Chungnam National University, Daejon 305-764, Korea
[4]Department of Earth Sciences, Busan National University, Busan 609-735, Korea
E-mail: hallman@casa.colorado.edu, ryu@canopus.chungnam.ac.kr, kang@uju.es.pusan.ac.kr, twj@msi.umn.edu

ABSTRACT

We introduce a method of identifying evidence of shocks in the X-ray emitting gas in clusters of galaxies. Using information from synthetic observations of simulated clusters, we do a blind search of the synthetic image plane. The locations of likely shocks found using this method closely match those of shocks identified in the simulation hydrodynamic data. Though this method assumes nothing about the geometry of the shocks, the general distribution of shocks as a function of Mach number in the cluster hydrodynamic data can be extracted via this method. Characterization of the cluster shock distribution is critical to understanding production of cosmic rays in clusters and the use of shocks as dynamical tracers.

Key words : cosmology: large scale structure – shock waves – synthetic observations

I. INTRODUCTION

In astrophysical environments generally, evidence of shocked gas is often reported (e.g. Markevitch et al. (2002)). Shocks develop due to locally supersonic gas flows during the process of large-scale structure formation. The gas is accelerated by the action of gravity in the potential wells of clusters, filaments and sheets. Shocks result in heating and compression of the gas in relatively small spatial regions. Therefore, the magnitude of the thermal emission jumps across the shock, and creates observable features. These features occur in clusters in observations of thermal X-rays. Because shocks are generated by not just relatively steady accretion, but by transient merging phenomena, we can trace the process of structure formation by reading the X-ray substructure in clusters.

Shocks are largely responsible for the conversion of gravitational potential energy to thermal energy in large-scale structure formation. However, shocks generate not only thermal dissipation, but are likely sources of accelerated particles. Studies have shown that a significant fraction of the incident kinetic energy at shocks can be converted into cosmic rays via diffusive shock acceleration (Kang & Jones, 2002). So, in addition to their use as tracers of dynamics in clusters, shocks also are efficient phenomena for the generation of cosmic rays. It is also possible that the cosmic ray population may contribute a dynamically significant pressure to the gas in clusters (Miniati, 2000).

In order to understand the role of accelerated particles in clusters, and explore the use of shock features as dynamical tracers, it would be useful to develop observational techniques which can sample not just obvious shocks, but the full range of shocks throughout the cluster volume. Simulations show that a complex web of shock surfaces are present in the gas of most clusters. Our goal is to determine how to identify and characterize these shocks observationally. The questions we address in this analysis are the following:

1. What is the observable distribution of shocks as a function of Mach number in simulated clusters?
2. Is the observed distribution an accurate reflection of the shocks in the cluster gas?

II. DATA ANALYSIS

(a) Cosmological Simulation

The parameters of the LCDM (cold dark matter with cosmological constant) simulation are as follows:

- $h = H_o/(100km\ s^{-1}Mpc^{-1}) = 0.7$
- total mass density $\Omega_M = 0.27$
- dark energy density $\Omega_\Lambda = 0.73$.
- baryonic mass density $\Omega_b = 0.043$
- normalization of matter power spectrum $\sigma_8 = 0.8$

The computational box consists of 1024^3 cells and 512^3 dark matter particles. The simulation environment is a comoving $(50h^{-1}Mpc)^3$ volume. For the hydro code, this gives a length resolution of $48.8h^{-1}$kpc. The simulations use a grid based cosmological hydrodynamic code developed by Ryu et al. (1993).

Proceedings of The 3rd Korean Astrophysics Workshop on *Cosmic Rays and Magnetic Fields in Large Scale Structure*

(b) Identification of Clusters/Groups

The cluster volumes are selected around centers identified as local peaks in the gas density. It is important to note that even the largest clusters in the simulation are a few times 10^{14} solar masses, and kT values of about 2.5 keV. These are relatively small by observational standards, and the distribution is a results from the relatively small physical volume simulated. This simulation was run to highly resolve the regions outside clusters particularly, and to resolve the regions near cluster cores better than previous work done with similar computational methods.

(c) Identification of Shocks in Simulation Data

The simulation code itself has been designed to capture shocks within a few zones, and adapted in other versions to explicitly inject and track the distribution of accelerated particles at shocks. As the simulation runs the Riemann solver detects and characterizes the shocks. In order to do a post-processing analysis of the type done in Ryu et al. (2003), we have done 1024 one-dimensional passes covering the entire plane of the simulation box along each of the three simulation grid axes. The following criteria are used to tag a zone as shocked:

1. $\Delta T \Delta s > 0$, the gradients of temperature and entropy are in the same direction
2. $\nabla \cdot v < 0$, The velocity divergence is negative, indicating a converging flow
3. $|\Delta logT| \geq 0.11$, The jump in temperature is above some specified value as defined by a scheme which differences the temperature in the i-1 and i+1 zones. In this case the value corresponds to a Mach number of 1.3.

The code typically captures shocks in 2-3 zones, so in each pass, the center of the shock is identified as the zone with the minimum velocity divergence. This zone is then assigned a Mach number calculated from the Rankine-Hugoniot jump conditions for a gamma law gas using:

$$M = \sqrt{\frac{8\frac{T_2}{T_1} - 7 + \sqrt{(8\frac{T_2}{T_1} - 7)^2 + 15}}{5}} \quad (1)$$

T_2 and T_1 are the postshock and preshock temperatures representing the minimum and maximum temperatures across the extent of the continuous one dimensional extent of each shock. Shock centers identified in more than one pass are assigned the maximum Mach number found. A minimum Mach number of 1.5 is used to avoid contamination from adiabatic features in the flow. The minimum pre-shock temperature used in this analysis is 10^4K, using the assumption of full photo-ionization of the low temperature gas.

(d) Synthetic X-Ray Observations

We use the physical values of temperature and density, and the MEKAL (Mewe et al., 1985) model, to generate a spectrum of X-ray emission at each grid location. The major thermal emission mechanisms are bremsstrahlung, and continuum and line emission from the most abundant atomic species. The chemical abundance is assumed to be Z = 0.3. We integrate the emissivities along each line of sight in the optically thin limit. The ray-tracing code that performs these operations is detailed in Tregillis (2002). The end result of the synthetic observation code is a set of images in chosen energy bands, spatially resolved to the level of the simulation data. A temperature map of each object and orientation can be generated by spectral fitting at each sky pixel of the images. A new feature of the SYNTH code added in this work (originally developed by Tregillis (2002) and modified for use on cosmological data by Miniati (2000)), is the use of instrumental characteristics to generate images as they would appear to real X-ray instruments. To correctly determine the broadband surface brightness, as well as the observed spectrum, we also include photoelectric absorption of X-rays along the line of sight using the Wisconsin absorption model (Morrison & McCammon, 1983) for a typical column depth of hydrogen along a line of sight to the selected redshift of the synthetic observation.

(e) Shock Finding in Synthetically Observed Images

The presence of a shock creates a jump in temperature and density across the shock surface. This leads to a jump in the thermal emissivity across the shock. Using synthetic X-ray images combined with the spectral temperature generated by fitting the spectrum at each sky location in the images, we do a blind search for shocks. This is similar to the method used in the simulation data, but we have only projected quantities to work with. Initially, I use the entire image plane to search for shocks. Since with the synthetic observations, we have unlimited sensitivity, this is possible. In reality it is necessary to look at the count rates which our simulated cluster would generate in a particular instrument in a reasonable exposure time in order to correctly gauge the observability of each cluster and individual features. Initially, however, it is useful to characterize the two-dimensional projected distribution of shocks deduced from observable quantities. The method used to identify shocks in the images uses criteria analogous to the three-dimensional technique from the previous chapter. Successive one dimensional passes through the image plane check the criteria

- ΔT $\Delta\sigma > 0$, the gradients of the spectral temperature and surface brightness are in the same direction
- $|\Delta logT| \geq 0.11$, same as for 3-d case, the temperature jump must be greater than a threshold

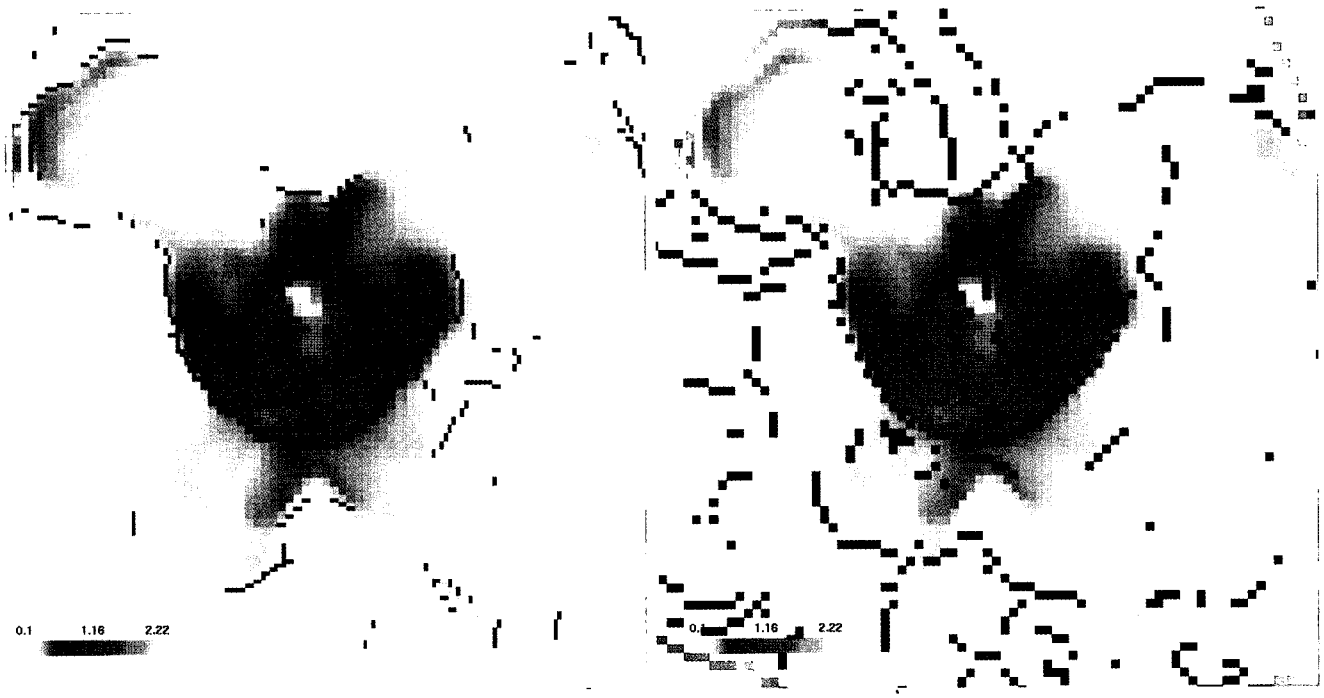

Fig. 1.— Synthetic X-ray observation of Cls3. Color shading is MEKAL weighted temperature. Overlaid black pixels are locations of shocks. Left panel is from synthetic observation identification, right is a slice through the cluster volume of shocks identified via the full three dimensional post-processing analysis. Color scale is shown. Physical scale is $(6.25h^{-1}Mpc)^2$.

corresponding to M = 1.3.

to determine whether a pixel lies within a shock. Then, as in the three-dimensional case, the shock center is identified. We have identified the middle of the continuous one-dimensional extent of zones identified as shocked as the shock center. Pixels identified as shock centers in both passes are assigned the higher Mach number of the two. The Mach number is calculated from the central difference of the projected temperature. This calculation is similar to what is done using observational data from real clusters (e.g. Kempner et al. (2002); Markevitch & Vikhlinin (2001)). In cases where the orientation of cluster features are somewhat obvious, an attempt is usually made to account for the projection effect of gas along the line of sight in order to more accurately measure the temperature jump (e.g. Markevitch et al. (2002)). We use a minimum jump in temperature associated with a shock of M=1.3 with this method to attempt to capture more weak shocks which might be seen obliquely in each projection. Errors in any spectral temperature calculation in many cases would preclude detecting jumps smaller than this.

III. RESULTS

An example of identified shocks in a simulated cluster is shown in Fig. 1. The left panel shows in gray and black the location of identified shock centers using the synthetic observation method. The color underlying is the calculated spectral temperature for this synthetic observation. On the right is the same spectral temperature image, this time overlaid with the locations of shock centers as found in a slice of the simulation hydrodynamic data near the center of the cluster. The correspondence between the shocks identified in the simulation data and in the synthetic observations is good, even using this simple approach.

Figure 2 shows the number of shocks per unit logarithmic Mach number interval for the synthetic observational shock finding method with a minimum surface brightness consistent with detection by the XMM-EPIC pn detector. The shocks are identified in synthetic observations of 3 orthogonal projections of all of the 10 most massive clusters/groups in the simulation at z=0. The dotted line represents the counts for the three-dimensional shock finding analysis for the gas in those same cluster volumes which is hotter than 10^7 K. This is a comparison of the relative proportion of shocks as a function of Mach number which exist in the hydrodynamic data with the shocks identified via the synthetic observations. We also should note that at the low Mach number end of the distribution, we should undercount shocks, since those shocks with a Mach number near the threshold could easily be missed when viewed at most orientations other than edge-on to the line of sight. In general, it appears the 2d analysis presents an accurate picture of the relative number of shocks as a function of Mach number. Both distributions cut off at M = 3-4. Projection effects should also lead to a lower maximum Mach number detected via

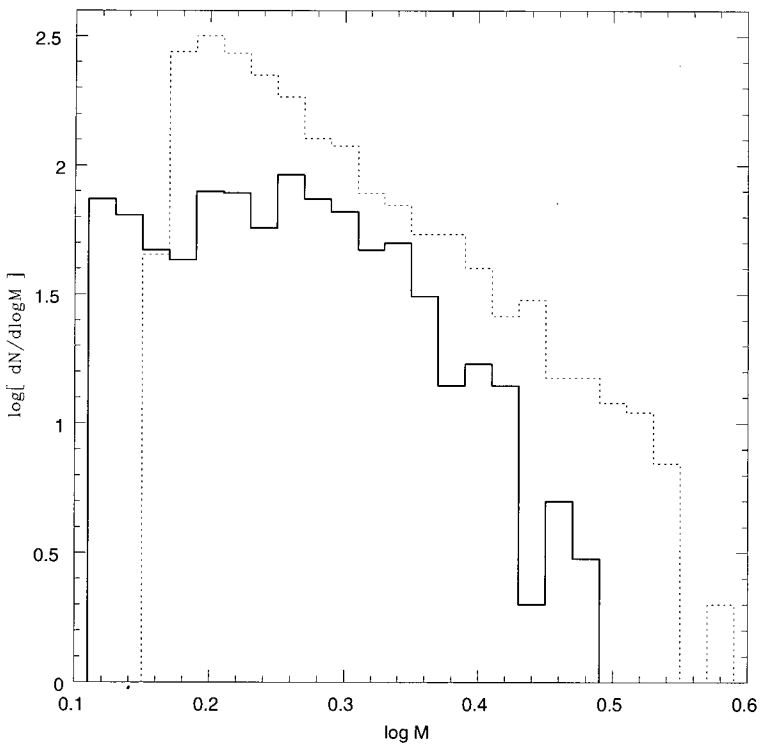

Fig. 2.— Comparison of number of shocks per logarithmic Mach number interval found using 2d and 3d methods. Solid line represents shocks identified in synthetic observational analysis. Dotted is for shocks identified in analysis of simulation data for shocks in cluster volumes in hot phase.

the synthetic observations than that in the simulation data.

IV. CONCLUSIONS

We have identified the location of possible shocks in synthetic X-ray observations of simulated clusters of galaxies. We use a simple blind search method to identify shocks using the synthetic observation data. Features identified in this way show excellent correlation with the location of shocks in the simulation hydrodynamic data. This simple approach allows for the identification of a large number of shock surfaces in each cluster or group, which leads to a better understanding of the real distribution of these features in clusters. Although we may underestimate the real shock strength due to projection effects, overall the distribution of shocks as a function of Mach number in clusters is well represented by the results of such a simple, systematic search of the image plane. In future work, we will examine the effectiveness of this method using realistic X-ray photon counts and errors in typical X-ray observations.

ACKNOWLEDGEMENTS

DR was supported in part by a grant of the Chungnam National University 2004 R&D Project. HK was supported in part by KOSEF through Astrophysical Research Center for the Structure and Evolution of Cosmos (ARCSEC).

REFERENCES

Kang, H. & Jones, T. W. 2002, Journal of Korean Astronomical Society, 35, 159

Kempner, J. C., Sarazin, C. L., & Ricker, P. M. 2002, ApJ, 579, 236

Markevitch, M., Gonzalez, A. H., David, L., Vikhlinin, A., Murray, S., Forman, W., Jones, C., & Tucker, W. 2002, ApJ, 567, L27

Markevitch, M. & Vikhlinin, A. 2001, ApJ, 563, 95

Mewe, R., Gronenschild, E. H. B. M., & van den Oord, G. H. J. 1985, A&AS, 62, 197

Miniati, F. 2000, Ph.D. Thesis

Morrison, R. & McCammon, D. 1983, ApJ, 270, 119

Ryu, D., Kang, H., Hallman, E., & Jones, T. W. 2003, ApJ, 593, 599

Ryu, D., Ostriker, J. P., Kang, H., & Cen, R. 1993, ApJ, 414, 1

Tregillis, I. L. 2002, Ph.D. Thesis